HIGH POWER S-BAND VACUUM LOAD

Final Report for STTR Project Starting 2/20/2012, ending 12/21/2015

Small Business: Muons, Inc.

552 N. Batavia Avenue, Batavia, IL 60510

Principal Investigator: Michael Neubauer

Research Institution: SLAC NATIONAL ACCELERATOR LABORATORY

2575 Sand Hill Road, Menlo Park, CA 94025 Under CRADA 13-206C Modification No. 1

Research Inst. PI: Anatoly Krasnykh

Approved for public release; further dissemination unlimited. (Unclassified Unlimited)

PREPARED FOR THE UNITED STATES DEPARTMENT OF ENERGY

Work Performed Under grant DE-SC0007559

SBIR/STTR RIGHTS NOTICE

These SBIR/SITR data are furnished with SBIR/SITR rights under Grant No DE-SC0007560. For a period of four (4) years after acceptance of all items to be delivered under this grant, the Government agrees to use these data for Government purposes only, and they shall not be disclosed outside the Government (including disclosure for procurement purposes) during such period without permission of the grantee, except that, subject to the foregoing use and disclosure prohibitions, such data may be disclosed for use by support contractors. After the aforesaid four-year period, the Government has a royalty-free license to use and to authorize others to use on its behalf, these data for Government purposes, but is relieved of all disclosure prohibitions and assumes no liability for unauthorized use of these data by third parties. This Notice shall be affixed to any reproductions of these data in whole or in part. (End of Notice)

Table of Contents

Table of Contents	2
ABSTRACT	2
Project Overview	3
Concept	4
Technical Milestones	4
Compression Ring Assembly	
Fabrication of the Lossy Ceramic Rings	
Fabrication and Assembly of the Compression Ring	
Assembly of the Compression Ring	7
RF Measurements	
TE10 to TE01 adapters	
Moveable Short	9
Graphic Showing Final Design with SLAC section	10
Measurements	10
MeasurementsFinal Design	12
Cooling	12
Commercialization Expertise	13
References	13
Internal Report 1: Dielectric Properties of Cold Test Toroid Assemblies v	
Internal Report 2: Summary of 2 Toroid Simulation vs. Cold Test Measur	

ABSTRACT

Through a combination of experimentation and calculation the components of a novel room temperature dry load were successfully fabricated. These components included lossy ceramic cylinders of various lengths, thicknesses, and percent of silicon carbide (SiC). The cylinders were then assembled into stainless steel compression rings by differential heating of the parts and a special fixture. Post machining of this assembly provided a means for a final weld. The ring assemblies were then measured for S-parameters, individually and in pairs using a low-cost TE10 rectangular to TE01 circular waveguide adapter specially designed to be part of the final load assembly. Matched pairs of rings were measured for assembly into the final load and a sliding short designed and fabricated to assist in determining the desired short location in the final assembly. The plan for the project was for Muons, Inc. to produce prototype loads for longterm testing at SLAC. The STTR funds for SLAC were to upgrade and operate their test station to ensure that the loads would satisfy their requirements. Phase III was to be the sale to SLAC of loads that Muons, Inc. would manufacture. However, an alternate solution that involved a rebuild of the old loads, reduced SLAC budget projections, and a relaxed time for the replacement of all loads meant that in-house labor will be used to do the upgrade without the need for the loads developed in this project. Consequently, the project was terminated before the long term testing was initiated. However, SLAC can use the upgraded test stand to compare the long-term performance of the ones produced in this project with their rebuilt loads when they are available.

Project Overview

S-Band vacuum loads at the SLAC linac are encountering operational problems, now that they have to operate under the stringent requirements of the LCLS: 50 MW peak power, 6 kW average power, and extremely tight phase stability for the linac. Muons, Inc. proposed a novel solution which incorporates mode conversion from TE10 in rectangular waveguide to TE01 in round waveguide, where lossy material is placed in the round waveguide and the selection of the TE01 mode minimizes the electric field normal to the surface of the lossy material.

This lossy material in the TE01 round waveguide is mechanically confined in compression (without brazing), in order to eliminate operationally induced tensile stresses in the lossy material. The wrap-around mode converter is based upon the X-band mode converter invented at SLAC, and the TE01 waveguide load design is based upon HOM load designs developed by Muons, Inc.

In Phase I of this project, a novel lossy ceramic material and a mechanical system for incorporating it into an S-band dry load were designed and tested. The lossy ceramic components were cast into cylinders and other novel shapes from slurries composed of mixtures of SiC and porcelain and processed to full densification and vitrification. The microwave characteristics of the lossy ceramic cylinders were measured to determine the optimum mixture for various elements of the load.

During Phase II, the manufacturing of components with the lossy ceramic material was studied to find the optimum design for low-cost manufacturing of the complete load. Through a combination of experimentation and calculation the components of a novel room temperature dry load were successfully fabricated. These components included lossy ceramic cylinders of various lengths, thicknesses, and percent of silicon carbide (SiC). The cylinders were then assembled into stainless steel compression rings by differential heating of the parts and a special fixture. Post machining of this assembly provided a means for a final weld. The ring assemblies were then measured for S-parameters, individually and in pairs using a low-cost TE10 rectangular to TE01 circular waveguide adapter designed and built to be part of the final load assembly. Matched pairs of rings were measured for assembly into the final load and a sliding short designed and fabricated to assist in determining the desired short location in the final assembly.

The plan for the project was for Muons, Inc. to produce prototype loads for long-term testing at SLAC. The STTR funds for SLAC were to upgrade and operate their test station to ensure that the loads would satisfy their requirements. Phase III was to be the sale to SLAC of loads that Muons, Inc. would manufacture. Unfortunately for Muons, an alternate solution that involved a rebuild of the old loads, reduced SLAC budget projections, and a relaxed time for the replacement of all loads meant that in-house labor will be used to do the upgrade without the need for the loads developed in this project. Consequently, the project was terminated before the long term testing was initiated. However, SLAC can use the upgraded test stand to compare the long-term performance of the ones produced in this project with their rebuilt loads when they are available.

Concept

From the inception of the project, the idea was to fabricate, in a simple manner, the lossy ceramics and machine them as little as possible. It was though this would keep the costs down. Only the outer diameter (to allow them to be compression fit within their vacuum sleeve), and the ends of the ceramic cylinders would be machined. Though not machine them to a "particular" length. Each cylinder/sleeve assembly would them be measured and calculation would select the ~10 assemblies which would create the "best" load.

Technical Milestones

The final chemistry of the lossy dielectric material was determined during Phase I of this program and is shown in Figure 1. Manufacturing techniques were modified from Phase I, where a casting process was used, to a hand wheel throwing technique where thicker rings could be fabricated and ground to final dimensions. The results are discussed in more detail in the section "Fabrication of the Lossy Rings".

The first task for Phase II was the construction of a stainless steel compression ring and design of an assembly process to make the compressed ring assembly. This was accomplished after some experimentation. The results are shown in the section, "Compression Ring Assembly".

The second task was design and fabrication of new mode converters from the rectangular TE10 to round TE01 mode. This was accomplished and measurements made to confirm the integrity of the new mode converters. Construction costs were determined to be less than half of the Phase I style mode converters. These results are discussed in the section, "RF Measurements: TE10 to TE01 adapter".

The third task was to measure the compression ring assemblies with the new mode converters, discussed in the section, "RF Measurements: Single Rings" and create matched pairs of rings, discussed in the section, "RF Measurements: Two Rings".

The final task was the construction of a moveable short to be used in measuring the VSWR of the final assembly and locate the optimum location of the short given the assembly of matched pairs of lossy rings. These results are discussed in the section: "RF Measurements: Moveable short".

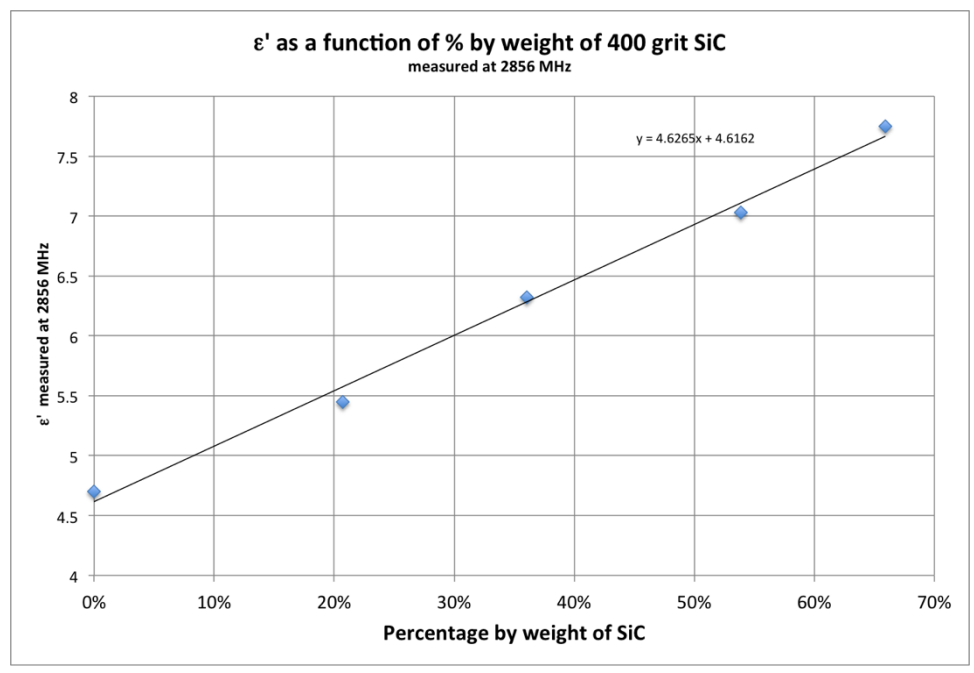


Figure 1. A linear fit between percentage by weight of a specific grit size of SiC in a ceramic clay and the measured dielectric constant of the material.

Compression Ring Assembly

Fabrication of the Lossy Ceramic Rings

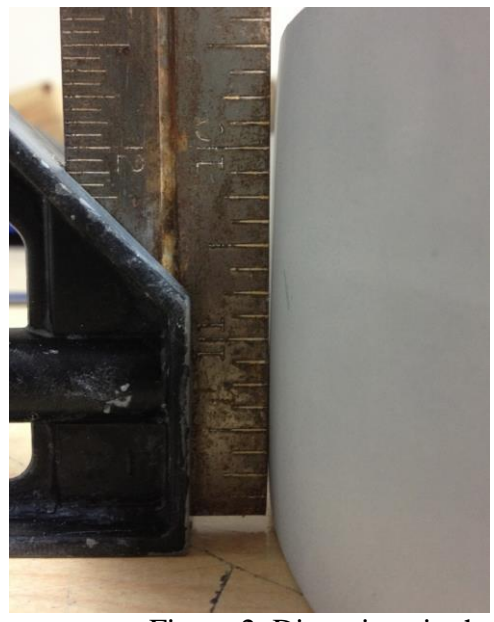




Figure 2. Distortions in the OD of the rings that were cast

During Phase I, a process was developed for making the lossy ceramic rings, but as work began on Phase II, distortions in the outer diameter of the cylinders required grinding the final

dimensions. This would have required that thicker rings be manufactured, thus the casting process needed to be reviewed. This led to the determination that a different manufacturing process was required. We accomplished that, making ceramic rings of varying thickness and lengths requiring only a final grinding of the OD to 6.000 +/-.001 inches. The ID was left untouched so we could have varying S-parameter measurements for various rings, and determine if the ID needed to be ground for strictly RF reasons.



Figure 3 Lossy ceramic rings prior to final ginding of the outside diameter.

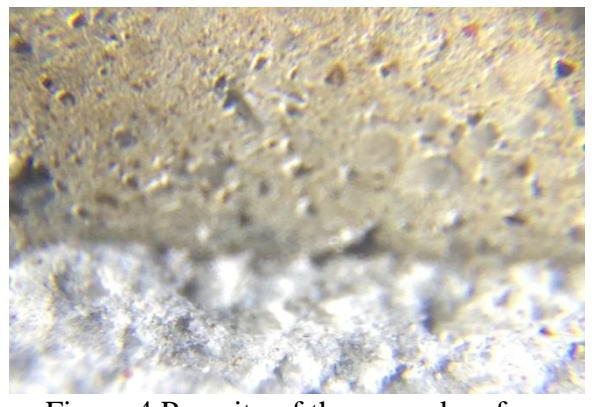


Figure 4 Porosity of the ground surface

There was some concern about the porosity of the material as shown in Figure 4. The solution for this type ceramic was an easy one. "Vac Seal" was purchased to coat the ceramic if it was found necessary to seal the surface. Subsequent analysis found that the pores were of a finite depth and would not create "virtual leaks". The amount/type of porosity is due to the temperature and length of time of the firing process. Higher temperature produces lower porosity. The firing temperature for the ceramics was 1200°C. With the compression rings and grinding of the final outer dimension, we did not believe porosity would lead to a problem for this type room temperature vacuum load, although we had a fix if required.

Fabrication and Assembly of the Compression Ring

The compression ring was machined from a hydroformed "top hat" made from stainless steel material that was 1/16 inch thick. We made the decision to proceed with a hydroformed part as opposed to machining from a cylinder or bar stock based on cost and process time. The rings produced from this process were adequate for the job as shown in Figure 5.





Figure 5. (a) A hydroformed "Top hat" from 304SS, (b) the cuts made to remove unwanted material.

Assembly of the Compression Ring

Several steps were experimented with and fixtures developed to accomplish the task of heating the stainless steel and cooling the ceramic. The interference fit was approximately 3-5 mils. A differential temperature between the parts of 320°C produced an easy assembly in the fixturing.

Modeling was performed in Comsol to determine the sleeve stresses and the proper design interference for room temperature. The Table below shows some results.

porcela	in - sleeve	thermal results	table			
			room temp.	total	in-band	at edge of torus
	model	sleeve thk (mils)	overlap (mils)	displacement (in)	v-M stress (MPa)	v-M stress (MPa)
	2D	50	5	0.001480	~240	418
	2D	50	3	0.000898	~145	252.3
	2D	68	5	0.001058	~240	433
	2D	68	3	0.000639	~145	261.4
	3D	50	5	0.001392	~230	280.3
	3D	50	3	0.000812	~145	162.1
	3D	68	5	0.000951	~215	293.3
	3D	68	3	0.000574	~145	177.1





Figure 6. (a) compression ring assembled with fixture. (b) ring assemblies s/n 012-017

RF Measurements

TE10 to TE01 adapters

A new style adapter was designed to minimize the cost, and two were made for S-parameter measurements. These adapters were discussed in the Continuation Report dated 1/24/2014. They were fabricated and testing began in September 2014. The test set is shown in Figure 7. The central cylinder is a ceramic / sleeve under test.

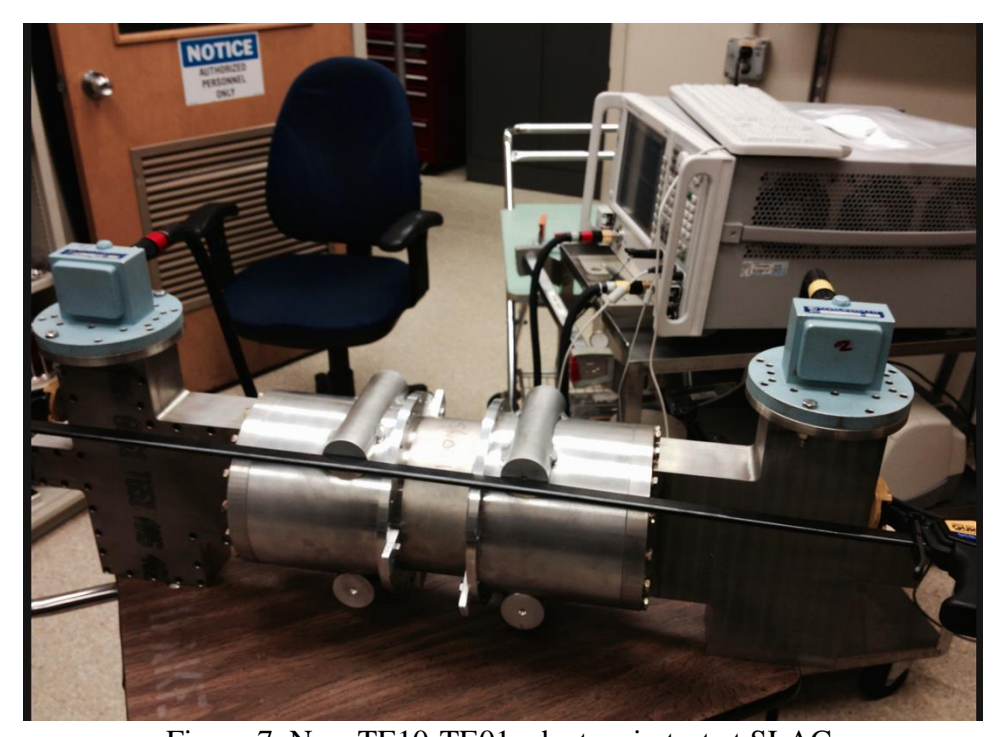
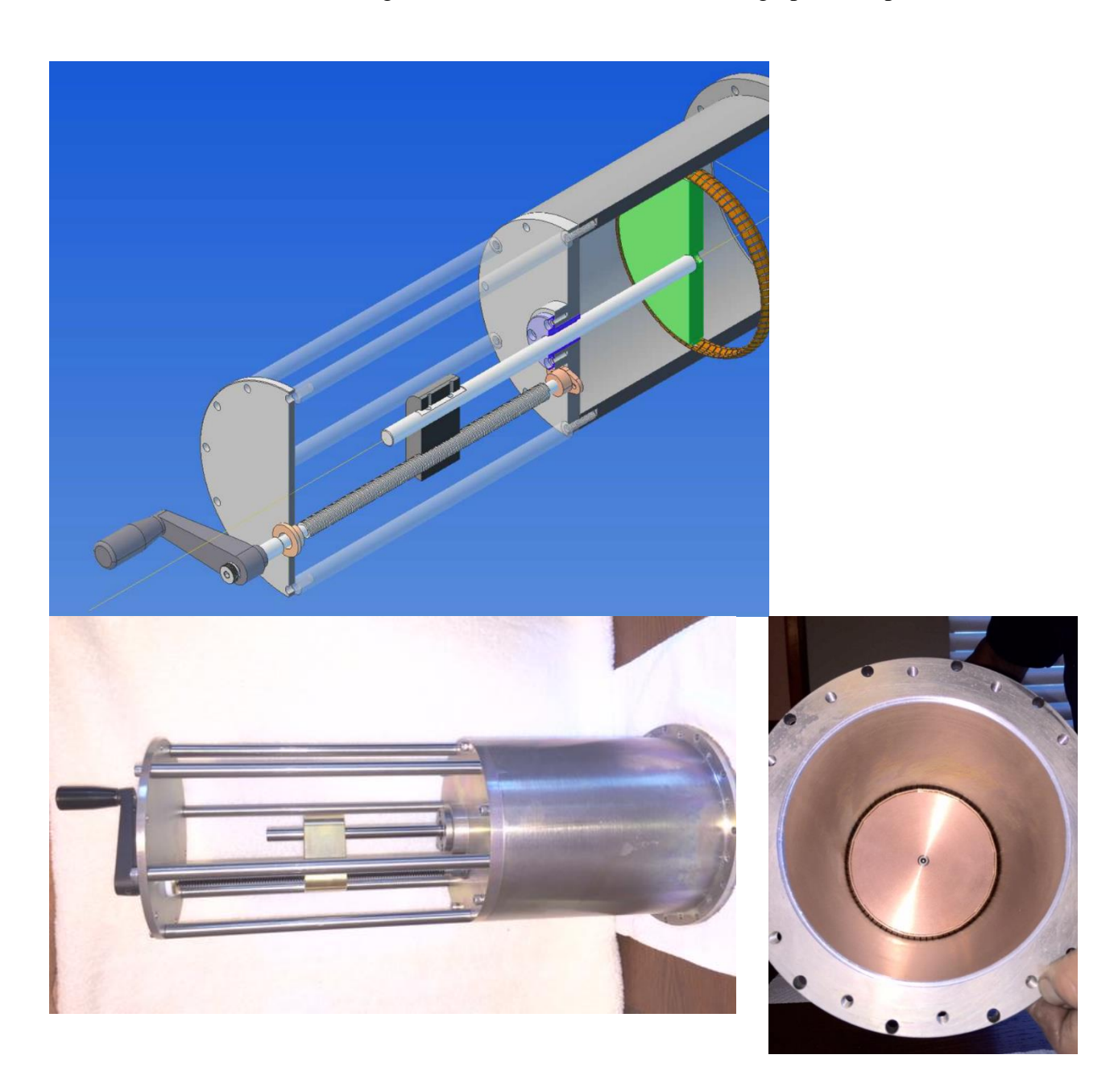


Figure 7. New TE10-TE01 adapters in test at SLAC.

Moveable Short

A Moveable Short was also designed and fabricated as shown in the graphic and photo below.



Graphic Showing Final Design with SLAC section

The graphic below shows how this type of load design might look integrated with a SLAC section. Note the cooling tubing which would surround each load section sleeve. In the prototyping and early deployment phase each section would have independent thermocouples to allow monitoring of the power deposition within the load sections. The "wagon-wheel" mode adapter shown is an earlier version that was replaced by the one shown in figure 7.



Measurements

Single Ring measurements were made as shown in Figure 7 for all 25 ceramic/sleeve assemblies manufactured to date. Double ring measurements were made as show Figure 8. The distance between the rings was adjusted to determine the spacing required for the reflection from the second ring to cancel the reflection from the first ring. We performed simulations and tests to learn the variables needed to create "matched pairs".

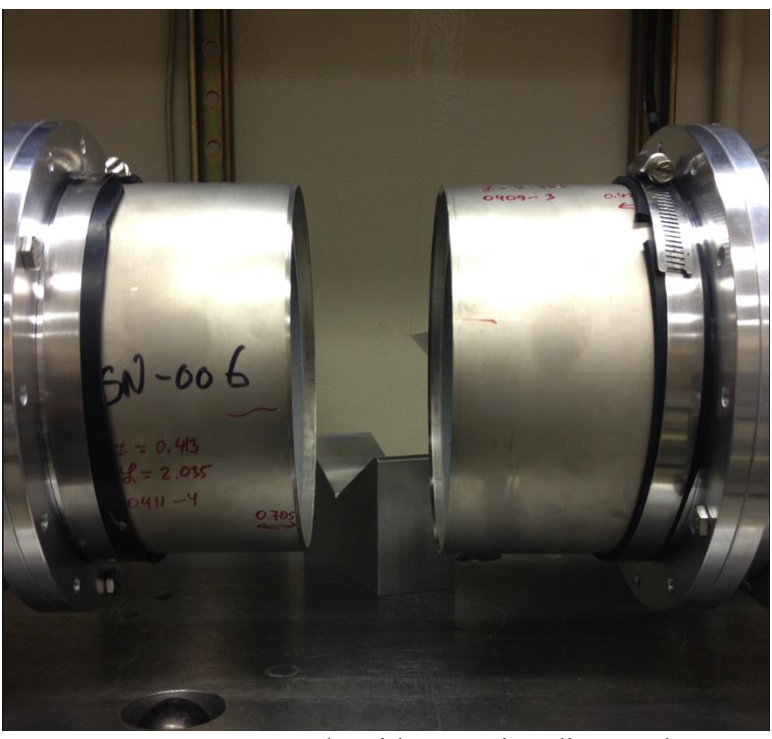


Figure 8. Two ring measurements were made with a varying distance between the rings to create a perfect match. (Shown without outer conductor "cover" for clarity.)

Finding the proper sequence of rings to produce a minimum VSWR was calculated from the data we had collected so far in the process. It was also possible calculate what dimensions would be needed to make single rings too, if we were not making matched pairs. Those calculations are shown in Figure 9.

0												
Input Watts	6000											
Watts per section	600											
		Forward	Watts	Backw	ard Watts			from Comso	l 1-toroid (2D)	simulations		
	db per			Input	watts	Total Watts				toroid length	material ε &	material
Section Number	section	Input Watts	watts lost	Watts	lost	per section		S21(dB)	toroid IR (in)	(in)	loss	sample
input coupler		6000										
1	0.46	5401	599		3 0	599		-0.4599	2.5236	3.0386	4.7-j*.1316	#1
2	0.51	4802	599		4 0	600		-0.5099	2.5075	2.9684	4.7-j*.1316	#1
3	0.58	4201	600		4 1	601		-0.5799	2.4856	2.872	4.7-j*.1316	#1
4	0.67	3603	599		5 1	600		-0.6701	2.4583	2.7503	4.7-j*.1316	#1
5	0.79	3004	598		6 1	600		-0.79	2.42134	2.5903	4.7-j*.1316	#1
6	0.96	2407	598		7 2	599		-0.96	2.36033	2.3489	4.7-j*.1316	#1
7	1.24	1810	597		9 3	600		-1.24	2.55362	2.6715	7.0-j*.2625	#41
8	1.73	1216	594	1	2 6	599		-1.7302	2.501	2.3508	7.0-j*.2625	#41
9	2.84	633	583	1	7 16	599		-2.84	2.24874	1.5376	7.0-j*.2625	#41
10	6.42	144	489	3	3 111	600		-6.4201	2.12789	1.5726	7.0-j*.2625	#41
short	16.18			144.43	4	5997	Total Loss					
	total one wa	y db loss										
						(a)						
						(a)						

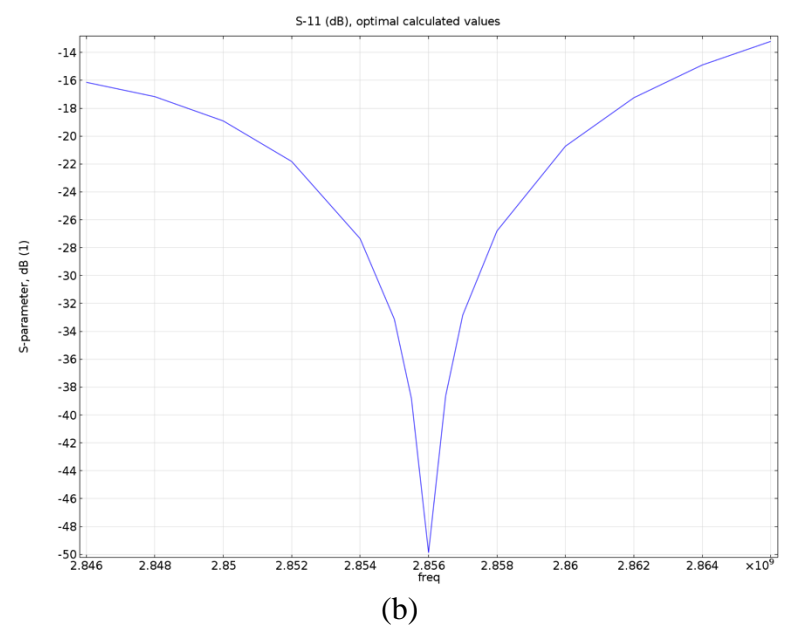


Figure 9. Calculations to determine size of the rings to make a perfect match using two different materials.

Final Design

The assembly of the final load had two approaches: a) combining 5 matched pairs, or b) ten compression ring assemblies fabricated to have specific S parameters and losses per ring. It was determined that combining 5 matched pairs had the more likely manufacturing likelihood than fabricating rings with specific S parameters and losses per ring. The Phase II effort was therefore focused on determining the parameters for making matched pairs from the twenty-five assemblies on hand.

Results of the measurements were compared to simulations run in Comsol. The concept being that once the simulation(s) could accurately predict the measurement results the 10-assembly load could be fully simulated prior to fabrication. As is often the case, "good" agreement between measurement and simulation is difficult to achieve.

Two internal reports were written discussing these efforts, and are copied in below (in their entirety as part of this Final Report.

Cooling

Cooling for the Hot Test prototype was planned to be accomplished by simply wrapping the final assembly with half inch copper tubing. Each ceramic/sleeve section could be individually wrapped and thermocouple. In that way we could monitor the power deposition in each of the ceramic/sleeve sections.

Some tests were conducted at Device Technologies to determine the force necessary to wrap the tubing around the cylinder, and work harden as well as deform the copper pipe flat against the compression ring assembly.

Commercialization Expertise

The commercialization for making the loads was planned to operate within Muons, Inc. We have access to the machine shop at Device Technologies in Yorkville, IL. They developed the processes for making the assemblies and have the capacity and expertise to make sufficient quantities for SLAC, should SLAC decide to use this type load to replace the coated rectangular waveguide loads that are deteriorating. With some additional equipment the process of making lossy ceramic rings can be increased in volume.

References

- 1) M. Neubauer, et. al., "S-Band Load Design for SLAC", 2013 PAC. accelconf.web.cern.ch/accelconf/pac2013/papers/wepho18.pdf
- 2) A. Krasnykh et al. "Overview of High-Power Vacuum Dry RF Load Designs" SLAC-PUB-16486. www.slac.stanford.edu/pubs/slacpubs/16250/slac-pub-16486.pdf

Internal Report 1: Dielectric Properties of Cold Test Toroid Assemblies via Simulation

For the SLAC S-Band Load project twenty-eight (28) ceramics loaded with SiC powder were formed and machined such that they could be "trapped" via thermal compression within a roughly 0.063" thick stainless steel sleeve, approximately 3" long. Each toroid was a different length and had different thickness. There was no effort to axially "center" the toroids along the length of the sleeves, so the amount of sleeve overhang on each side of any particular toroid is different.



Figure 10: Shown is a toroid compressively inserted into a steel sleeve.

Each toroid/sleeve assembly (TSA) was measured using two SLAC designed (Muons fabricated) Mode Converters (MCs), and Adapter rings which interfaced the MCs and the TSAs.

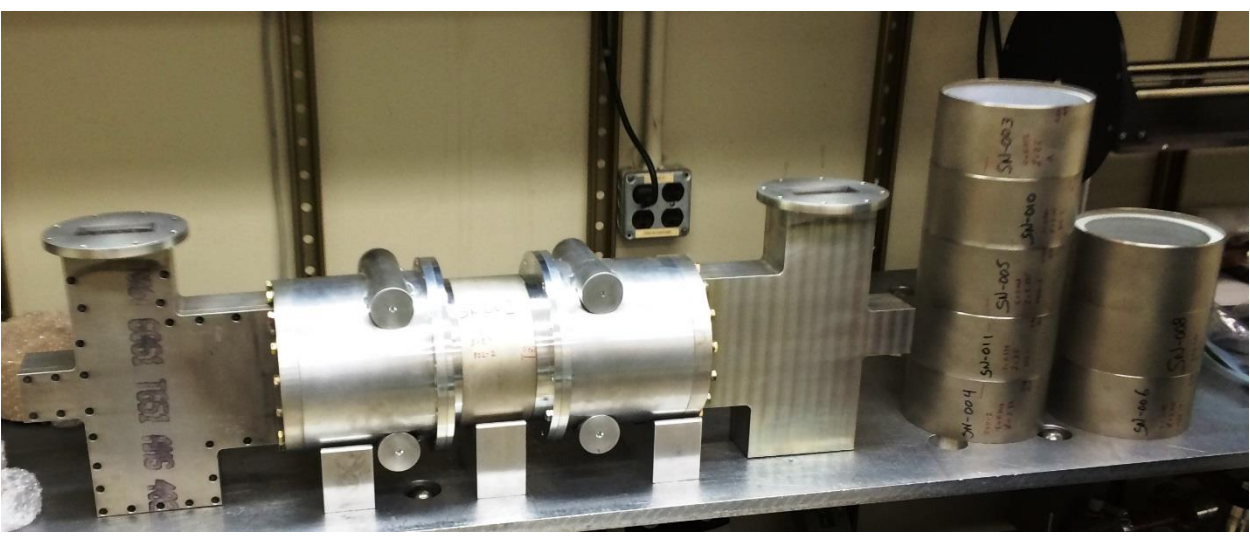


Figure 11: Cold Test measurement set-up at SLAC showing two Mode Converters, two Adapter Rings, and a Toroid/Sleeve Assembly in between.

Each of the 28 TSAs was measured in the Cold Test experimental set-up shown in Figure 11 using a Network Analyzer (NA). The S-parameters, namely S11 and S21 were measured and recorded.

The same Cold Test set-up was 3D modeled in Comsol as shown in Figure 12.

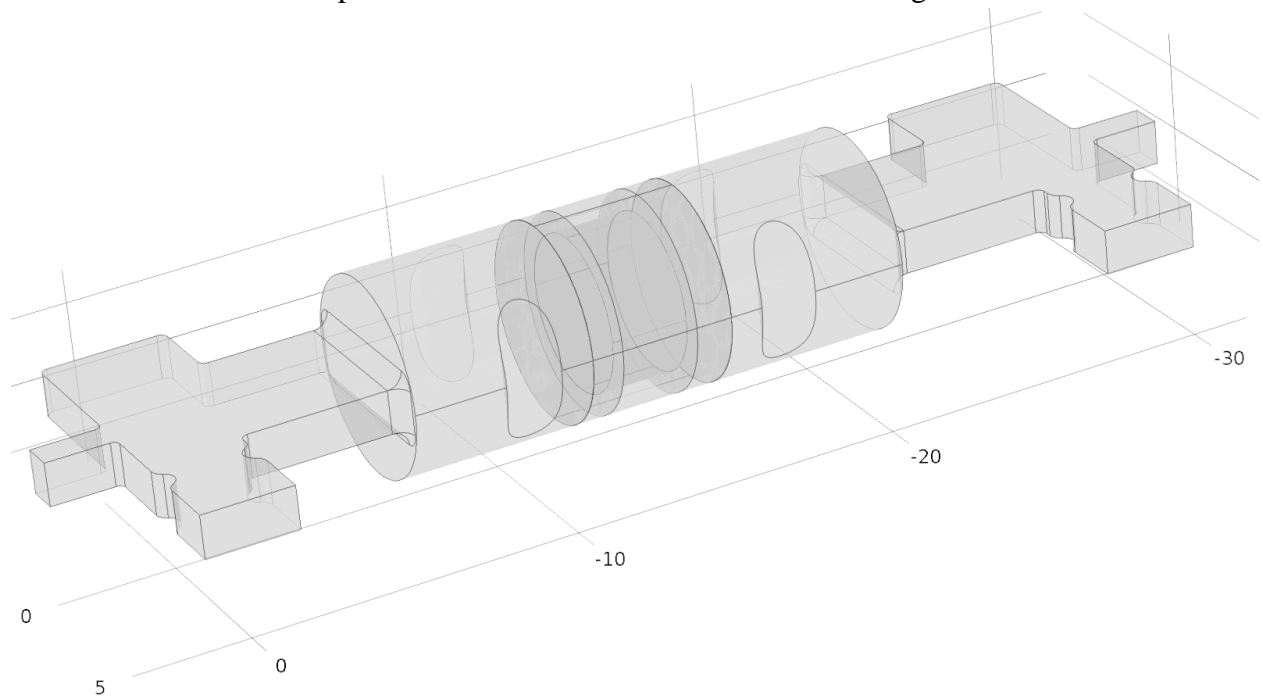


Figure 12: Comsol model of Cold Test measurement set-up for measuring the S-parameters of a Toroid/Sleeve Assembly.

By varying the dielectric parameters of the toroid material within the simulation, it was possible to determine what values of ε_r and $\tan\delta$ yielded identical S11 and S21 values as were measured in the Cold Test measurements. The Table on the last page of this report shows the results.

Explanation of Results Table

- TSAs 1 and 2 were the first assemblies fabricated and were measured in the first set of Cold Test measurements performed early in November 2014, in which TSAs 001 through 011 were all measured. These measurements were likely performed without the use of the Adapter Rings. I have no knowledge of the material composition (i.e. percentage of SiC mixed into the clay) of these two Toroids.
- TSAs 003 through 011 were re-measured along with the second group of fabricated TSAs (012 through 017) in mid December 2014. I have no knowledge of the material composition of Toroid 3.
- TSAs 004-011- were measured and simulated and the results are shown in the attached Table. NOTE 1: During the measurements, it was not recorded in what orientation the TSA was inserted into the Cold Test set-up. Since the amount of sleeve overhang differs on each side of the toroid, some simulation runs (005, 006, and 010) were performed twice (once in each TSA orientation). It can be noted that even with substantially differing amounts of overhang on each side of the toroid, the calculated values of ε_{T} and $\tan\delta$ determined did not differ substantially, but did differ.

NOTE 2: Not all of the TSAs were solvable. i.e. a match could not be found between the measured values of S11 and S21 and the simulated values of S11 and S21. This was the case for TSA 011.

- TSA 014 Is one of a group of TSAs (012 through 017) that were fabricated and delivered to SLAC at the same time. I have no knowledge of the composition of any of the 6 toroids in these Assemblies. TSA 014 is the only Assembly that we presently know the whereabouts. The other five TSAs are misplaced.
- TSAs 018 028 were the last batch of assemblies made and delivered to SLAC. They were Cold Test measured in early July 2015. The material compositions of all of these assemblies except 019, 023, and 025 are known. Assemblies 019 and 020 would not solve i.e. see NOTE 2 above. As can be seen in the Table 018, 026, 027, and 028 have two sets of "solved" values for the dielectric properties, with a comment, "other side

of S curve". In these cases a second set of dielectric parameter values were found which in the simulation also yielded identical S11 and S21 values as those which were measured during Cold Test. Note that for these particular TSAs the S11 and S21 measured values were of similar magnitude.

So, of the 28 TSAs currently fabricated there are only 14 that I can simulate in an effort to fabricate a multi toroid load assembly. And, one of those (014) I do not know the percentage of SiC in the composition.

	Α	В	С	D	Е	F	G	Н	1	J	K	L	M	
2														
3				SiC gms		toroid		toroid	sleeve	1-side				
4	S/N	s11, dB	S21, dB	in sample		length		thickness	length	gap				
5						(in)		(in)	(in)	(in)	ε,	tanδ	ε"	
6														
7	004	-9.759	-0.937	(100)		2.33		0.444	2.9	0.42	5.5106	0.0349	0.1921	unrealistic oth
8														
9	005	-10.719	-0.829	(100)		2.385		0.46825	2.99	0.425	4.6186	0.0415	0.1915	
10										0.18	4.5844	0.0421	0.1930	
11				_										
12	006	-11.906	-0.592	(100)		2.035		0.41325	2.9	0.705	4.3335	0.0567	0.2458	
13										0.16	4.2959	0.0576	0.2474	
14				_										
15	007	-10.107	-1.032	(100)		2.29		0.46825	2.99	0.455	6.7933	0.0186	0.1265	
16														
17	008	-9.92	-1.078	(200)		2.21		0.4195	2.99	0.45	5.5137	0.0639	0.3523	
18														
19	009	-10.008	-1.055	(200)		2.31		0.35825	2.99	0.455	7.5608	0.0533	0.4029	
20				,										
21	010	-13.92	-0.491	(200)		2.145		0.33075	2.99	0.6	4.8675	0.0942	0.4586	
22										0.245	4.7945	0.1015	0.4866	
23				r							,,,,,,,,,,,,,,,,,,,,,,,,,,,,,,,,,,,,,,,			
24	011	-15.504	-0.632	(200)		2.5		0.33875	2.99	0.24				won't solve
25							- 1							
26 27	014	10.005	0.507	?		2.22	ave_id	0.04	2.0	0.205	5.7000	0.0706	0.4406	
	014	-12.825	-0.587		£ 1 2 /1 7 /1 4	2.23	5.320	0.34	3.0	0.385	5.7008	0.0736	0.4196	
28	- green va	lues from A	anatory S II	ist (meas. o	1 12/1//14	1								
30		S11 (dB)	S21 (dB)	SiC gms				+ =ve		LS				
	018	-5.517		(300)		2		t_ave 0.563	3.000	0.27	8.2782	0.0256	0.2121	
32	018	-5.517	-3.251	(300)		2		0.505	3.000	0.27	10.9422	0.0357		other side of S-
	019	-10.567	-3.117	?		2.1		0.582	3.015	0.255	10.5422	0.0557	0.0511	Caner side of 5
	020	-10.208	-1.002	(100)		2.305		0.470	3.000	0.28				won't solve
	021	-2.717	-6.637	(300)		1.5		0.575	3.000	0.275				won't solve
	022	-6.227	-3.096	(300)		1.8		0.455	3.000	0.25	6.8108	0.0999	0.6801	no other side of
	023	-7.185	-3.648	?		1.95		0.685	3.000	0.25				
	024	-8.855	-1.16	(100)		1.91		0.378	3.005	0.125	6.8997	0.0623	0.4300	no other side of
	025	-9.468	-2.489	?		1.78		0.718	3.000	0.195				
	026	-4.237	-4.969	(300)		2.43		0.628	3.000	0.25	6.4979	0.0440	0.2858	
41											7.5870	0.0440	0.3338	other side of S-
42	027	-3.839	-4.866	(300)		2.34		0.638	3.005	0.255	6.6893	0.0377	0.2524	
43											7.6102	0.0389	0.2958	other side of S-
44	028	-4.754	-4.378	(300)		2.36		0.680	3.000	0.255	5.7326	0.0425	0.2434	
45											7.4877	0.0421	0.3154	other side of S-
46	- values fr	om Anatol	y on 7/6/1	5										

Internal Report 2: Summary of 2 Toroid Simulation vs. Cold Test Measurement Results

This has not been either a simple measurement to make using the fabricated parts, not one that was easily simulated in Comsol.

Just to determine the value of the dielectric properties (ϵ_r and $\tan\delta$) to use in the simulation was an effort. This required Cold Test measurements to be made at SLAC using the fabricated Mode Converters (MCs), various additional parts (adapters, "Vee" blocks, Sliding Short), and various Sleeve / Toroid Assemblies (STAs) to test, with each toroid being unique with regard to dimensions and composition, and each toroid being uniquely placed within its steel sleeve.

Determination of Dielectric Properties for each Sleeve / Toroid Assembly

Each unique STA was measured at SLAC using the following cold test set-up:

A Network Analyzer (NA) was used to supply the RF and to measure the S-Parameters, S11 and S21.

An identical 3D physical model was created in Comsol (shown in Figure 1), with sizes and spacings as accurate as possible.

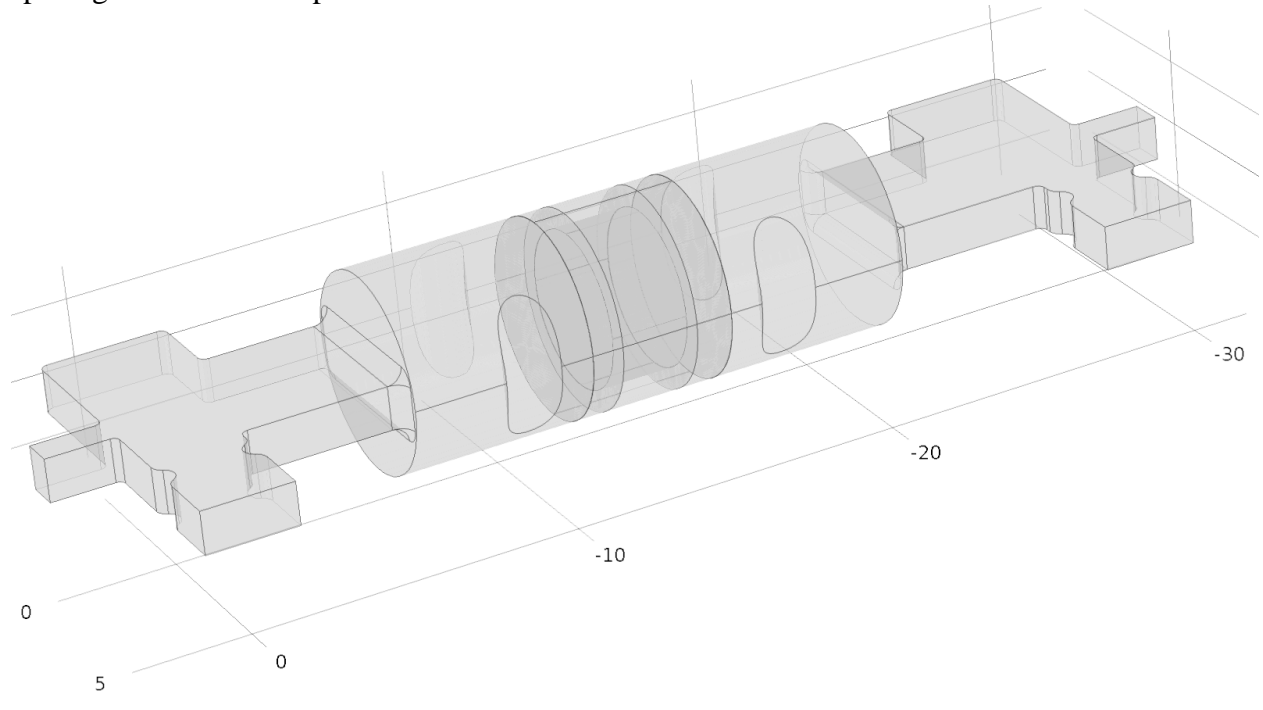


Figure 1: Comsol model for measuring single STAs.

A parameter study of ε_r and $\tan\delta$ was performed in the simulation to determine the exact values of these two variable which yielded the measured S11 and S21 values supplied by the SLAC measurements. The details of this parameter study are too cumbersome to mention here, but to determine one set of ε_r and $\tan\delta$ values for one STA required approximately 4 hours work. When STAs numbered 003 through 017 were tested it was not noted which-way-around the STA assembly was placed in the test set-up, thus the parameter study needed to be performed twice for each STA, once in each orientation. The result of turning around the STA in the simulation model, while not substantial, was small to moderate, and thus necessary to provide the best dielectric values for further simulation.

The parameter study mentioned above is not yet complete for all STAs. Indeed, no study has yet been performed for STAs 012 through 017, as all but 014 cannot be located.

Simulation of two SLAs and SLAC Cold Test Measurements of same

Our plan had been, that we would not attempt to fabricate (size and composition) each toroid "to spec", but rather would measure each STA to determine its unique dielectric properties. The recent two toroid test was an attempt to judge the efficacy of that approach.

STAs 005 and 006 were chosen as the two STAs with which to try this test. Both toroids were fabricated using a similar percentage of SiC (100 gms. per 4 lbs. of clay). The test was defined and after some initial difficulties with spacings and orientations of the STAs, SLAC measured the S11 and S21 values. Figure 2 shows the Comsol geometry for the simulation.

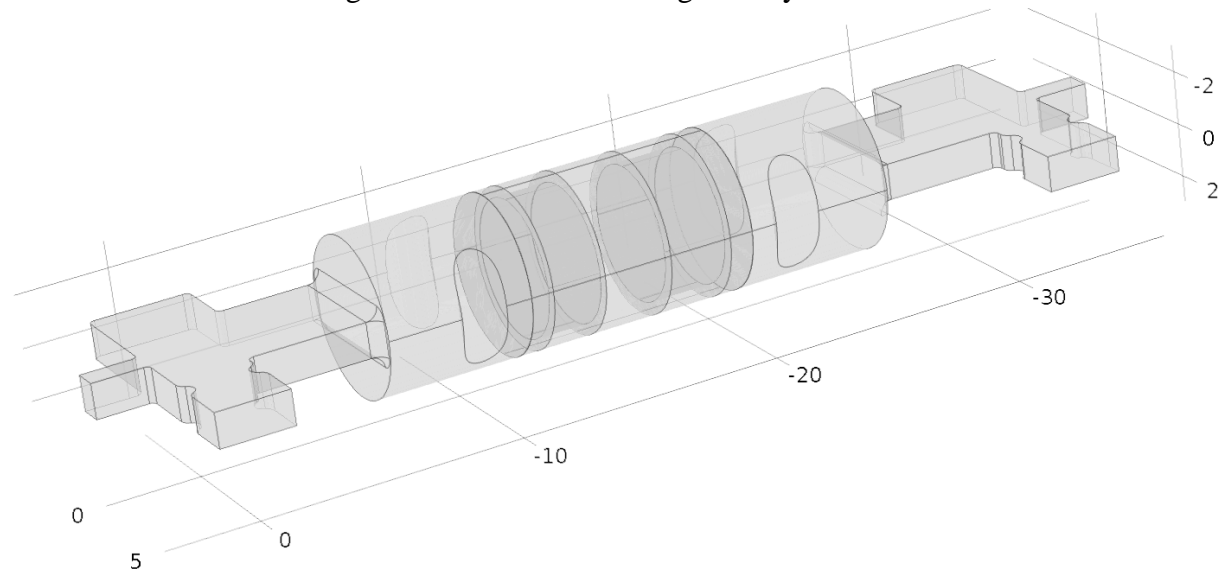


Figure 2: Comsol geometry for two SLAs simulation.

Using the method described above, the dielectric properties for toroid 006 were determined to be ε =4.3335 –j*.2458, and tan δ = .0567, and the dielectric properties for toroid 005 were determined to be ε =4.6186 –j*.1915, and tan δ = .0415.

The attached spreadsheet Table shows the dimensions and results from the two comparison runs.

Table 1: two toroid spacings and measurements and simulations results Table.

assy	adapter	sleeve	a1	sleeve	space	sleeve	a2	sleeve	adapter	S11 meas	S21 meas	S11 calc	S21 calc
	length	6a	toroid	6b	added	5a	toroid	5b	length	(swr)	(dB)	(dB)	(dB)
corr#1	0.688	0.16	2.035	0.705	1.12	0.415	2.385	0.19	0.688	2.167	-1.363	-7.530	-1.626
										-8.672 (dB)			
corr #2	0.688	0.16	2.035	0.705	1.48	0.415	2.385	0.19	0.688	1.008	-0.706	-15.777	-0.819
					2.6					-47.993 (dB)			

Anatoly's recent Results pdf indicates on page 4, "dZ_adapter=0.822". The parts drawing indicated that the adapter length should be 0.800", but this includes a 0.050" lip that should nest inside the MC's output flange, and the tapered male "mating" region on the opposite side. When these are taken into account the "effective" length (based on the piece part drawing) should be 0.688" which is what I used in the simulations.

The Table lists the distances (spacings) from the RF input side (on the left) toward the RF output side (on the right). Both the Cold Test measurement results and the Comsol simulation results are shown on the far right of the Table.

Corr #1 is for the toroid face separation of 1.12" i.e. the two sleeves were "mated". This is the value obtained when each of the sleeve overhangs is added together. Though I wonder, since the sleeves overlap due to the "nesting" chamfers, if the true toroid face separation should not be 1.120 - 0.063, or 1.057"? Nevertheless, the simulation was run with the 1.12" separation. The measured S11 value is -8.672 dB, and the simulation yields a S11 value of -7.530 dB. The measured S21 value is -1.363 dB, and the simulation yields a S21 value of -1.626 dB.

Corr #2 is for the toroid face separation of 2.6". The measured S11 value is -47.993 dB, and the simulation yields a S11 value -15.777 dB. The measured S21 value is -0.706 dB, and the simulation yields a S21 value of -0.819 dB.

I ran a parameter study varying the adapter length and the toroid separation by small amounts, to see if possible small distance (spacing) variations between the measurements and the simulation could account for the differences in the results. The answer is "NO". Small spacing variations on the order of ± 0.1 " only cause small differences in the calculated S-parameters. Not nearly enough to account for the amount of difference seen here.

Use of the Sliding Short

The output MC was removed and replaced with the recently fabricated Sliding Short (SS). So, now the cold test set-up appears as follows:

Input
$$RF - MC - adapter - STA - adapter - SS$$

In Comsol the geometry appears as in Figure 3.

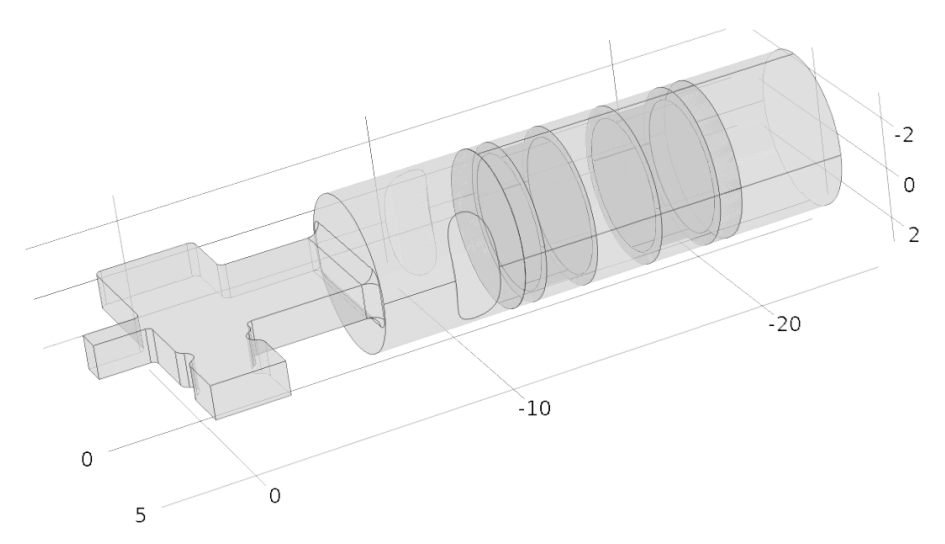


Figure 3: Comsol geometry for two toroid model with Sliding Short.

For the case where the spacing between the two toroid faces was 2.6", Anatoly made cold test measurements of S11 for a number of different positions of the SS. When the SS is part of the cold test measurement set-up it is not possible to "measure" the location of the Short relative to the toroids, rather an "external" measurement was substituted. Prior to assembly, Anatoly measured the correlation between the Short position, and the substitute measurement value, and are reported this on page 11 of the Results pdf. Unfortunately, the two measurements yielded two substantially different values which differed by 0.103". This could easily be correct, either due to backlash or wobble in the SS mechanism. Nonetheless, since it is quite easy to simulate both cases that is what I did. In Table 2 these values are called H₁ and H₂.

Table 2: Cold Test measurement and Comsol simulation results for the two toroid SLAs model using the Sliding Short.

Sliding Sh	ort	0.968	0.865														
	SS meas	depth of short		depth of short		depth of short		depth of short		epth of short sp bet torr		rr		S11 meas	S11 meas	S11	calc
	<u>B</u>	H ₁	H ₂	Δ	<u>A</u>			(swr)	(dB)	H ₁ (dB)	H ₂ (dB)						
	8.892	7.924	8.027	0.103	2.6			17.724	-0.981	-1.006	-1.012						
	5.932	4.964	5.067	0.103	2.6			13.792	-1.262	-1.247	-1.303						
	5.054	4.086	4.189	0.103	2.6			11.180	-1.558	-1.005	-1.010						
	4.13	3.162	3.265	0.103	2.6			13.239	-1.315	-1.326	-1.254						
	3.097	2.129	2.232	0.103	2.6			17.460	-0.996	-1.834	-1.857						
	2.127	1.159	1.262	0.103	2.6			12.809	-1.359	-1.246	-1.304						

The measurement and simulation results are shown on the right-hand side of the Table. The comparison between the measurements and simulation values seem reasonably close, except for those high-lighted in color. I can only surmise that there is some error for those two values.

I ran a parameterized study varying the "H" value of SS distance. The result is shown in Figure 4 below.

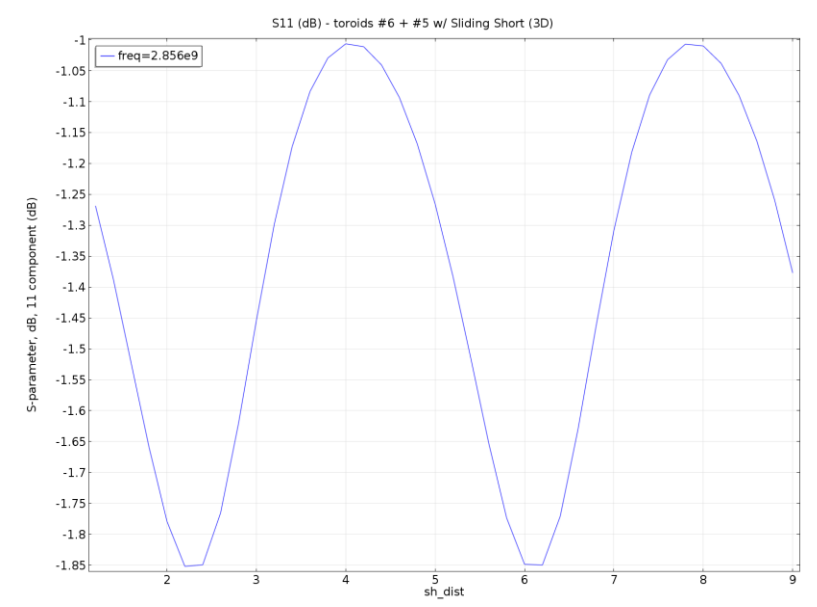


Figure 4: Two toroid Comsol simulation with varying Sliding Short position.

As can be seen, the simulation behaves as would be expected. However, if we graph the data of Table 2, we can see where the discrepancies occur. Figure 5 is that graph and shows that the measurement and the simulation results seem to be 180° out of phase. I do not understand why this would occur. Perhaps one of you has an idea?

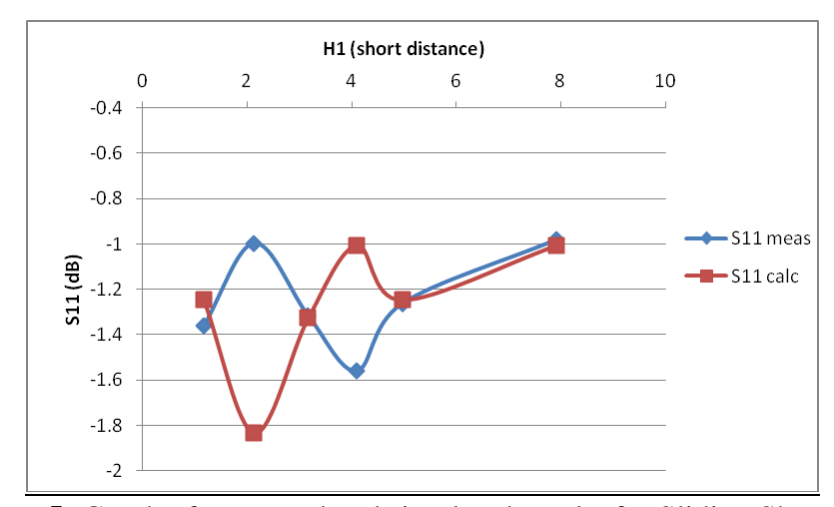


Figure 5: Graph of measured and simulated results for Sliding Short data.

Summary (Internal Report 2)

We were reasonably disappointed in the comparisons between the measurements and simulations for the case where both MCs are used and S11 and S21 are measured. However, the comparison of results for the case where the SS is used seems somewhat better, though I don't understand the seemingly 180° out of phase result.